Progress In Electromagnetics Research, Vol. 127, 15–30, 2012

AN ELECTRONICALLY CONTROLLABLE METHOD FOR RADAR CROSS SECTION REDUCTION FOR A MICROSTRIP ANTENNA

Y. P. Shang, S. Q. Xiao*, J. L. Li, and B.-Z. Wang

Institute of Applied Physics, University of Electronic Science and Technology of China, Chengdu 610054, China

Abstract—PIN diodes are used to electronically switch a rectangular microstrip antenna between the optimal radiation state and the low radar cross section (RCS) state in this paper. A useful loading circuit is proposed. The circuit is connected between the patch and the ground plane of the antenna at each loading position. The loading positions of the circuit are determined by studying magnitude distributions of the induced electric field and analyzing statistically how many times that the maximum electric field occurs in each area for each discussed incident angle. PIN diodes are equivalent to capacitances and resistances when diodes are reverse-biased and forward-biased, respectively. When the antenna is not in service and excited by an incident plane wave, obvious RCS reduction is realized. In addition, the radiation performances are well maintained when the antenna is in service for transmitting or receiving signals.

1. INTRODUCTION

Microstrip antennas have been widely used in kinds of military targets for they can be easily implemented on the surface of the target and have the characteristics of light weight, low profile as well as fitness for active integration [1, 2]. However, antennas, as efficient radiators of electromagnetic field, have been dominant contributors for the overall radar cross section (RCS) of low RCS platforms. Applying lossy superstrates above the microstrip patch [3, 4], using ferrite materials as antenna substrate and cover layer [5, 6] as well as distributed impedance loading [7] have been reported to reduce the RCS of microstrip antennas but at the expense of the gain and radiation

Received 22 February 2012, Accepted 27 March 2012, Scheduled 5 April 2012

* Corresponding author: Shao-Qiu Xiao (xiaoshaoqiu@uestc.edu.cn).

efficiency. Lumped resistance loading is also used for microstrip antennas RCS reduction [8, 9], but the RCS reduction occurs only for one given incident angles. RCS reduction is realized by using two circular apertures in the patch, a defected ground structure (DGS) and a shorting post with a gain decrease of 2.3 dB [10]. A reconfigurable Yagi-Uda substrate is put on the top of a patch antenna to reduce the RCS [11]. Cutting slots on the patch or the ground plane and using an FSS as the ground of a reflectarray antenna are used to realize the RCS reduction [12–16]. Besides, a varactor is used to tune the scattering response of a circular microstrip patch antenna [17], but the radiation efficiency is obviously impacted. Scattering from a narrow strip dipole antenna loaded with a PIN diode has been investigated [18], but the radiation performance is not discussed. These reported results indicate that the obvious RCS reduction of a microstrip antenna without sacrificing its radiation performances for all incident angles within all frequency bands is hard and challenging.

Recently, the electronically controllable method was proposed to adjust dynamically antenna radiation performances by using switchable devices [19–22], which exhibits extensive application prospect of switchable technique in antenna design. In this paper, an electronically controllable method is proposed to realize RCS reduction of a microstrip antenna by using PIN diodes. The optimal loading positions of PIN diodes are determined by analyzing mode distributions of the induced electric field. The antenna can be switched between the low RCS state and the optimal radiation state in order to realize a good compromise between the obvious RCS reduction and the optimal radiation performance.

2. DESIGN OF THE REFERENCE ANTENNA

A reference microstrip antenna with probe-fed rectangular patch is designed and depicted in Fig. 1. The coordinate system shown in Figs. 1(a) and (b) is used and its origin is at the center of the patch. The antenna is designed at the operating frequency of 2.5 GHz for study. The dielectric substrate has a relative permittivity of $\varepsilon_r = 2.33$ with loss tangent $\tan\delta = 0.0012$ and a thickness of $h = 3.6$ mm. The size of the patch is $L \times W = 35.95\,\text{mm} \times 47\,\text{mm}$. The size of the ground plane is $LG \times WG = 57.25\,\text{mm} \times 71\,\text{mm}$. The feed point on the patch is $(x_f, y_f) = (-8.5\,\text{mm}, 0\,\text{mm})$. As shown in Fig. 1(c), the realized gain of the antenna is about 7.71 dBi, the relative bandwidth with S_{11} less than -10 dB is about 4.2%. In this paper, the antenna performances are simulated by using Ansoft HFSS 10.0 which is based on finite element method.

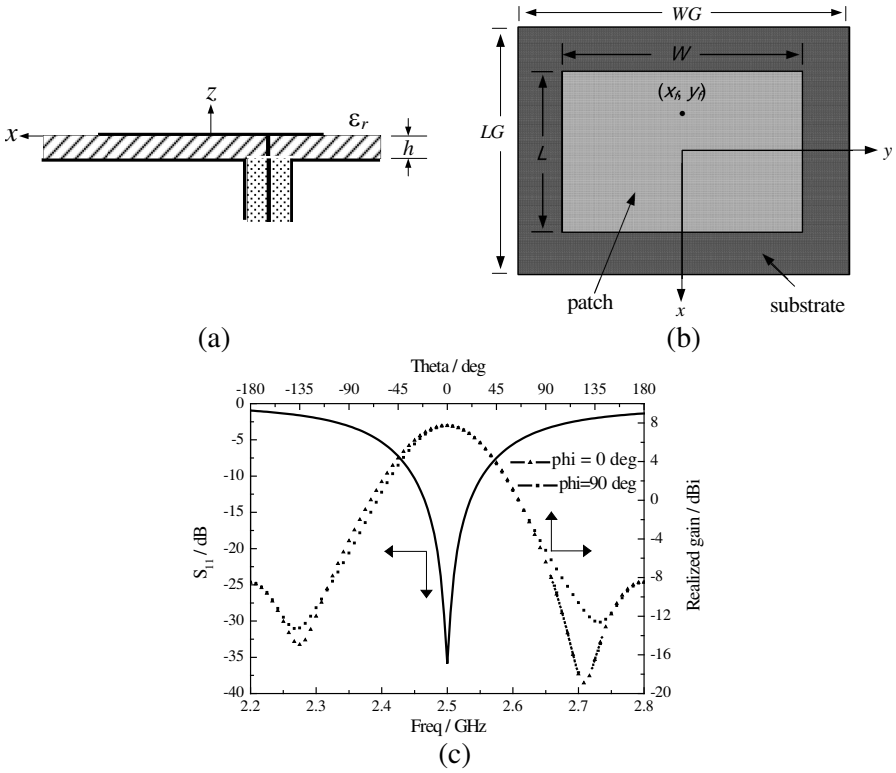

Figure 1. Reference antenna and simulated radiation performances. (a) Side view. (b) Top view. (c) Realized gain at 2.5 GHz and S_{11}.

3. RCS REDUCTION DESIGN OF THE ANTENNA

3.1. Bias Circuit for PIN Diodes

As it is well-known, the PIN diode appears as a variable RF-resistance when it is forward-biased and appears as a capacitance when it is reverse-biased [23]. Two cascaded PIN diodes (P_1 and P_2) are used at each loading position in order to increase the total forward-biased resistance and reduce the total reverse-biased capacitance. The selected direct current (DC) bias scheme is shown in Fig. 2. To decouple the bias loop and RF path as well as to isolate two diodes, capacitors C_1, C_2 and C_3 are used. The circuit is connected between the patch and the ground plane. During the process of simulation, two cascaded PIN diodes (P_1 and P_2) are equivalent to lumped resistances R_{eq1} and R_{eq2} when they are forward-biased and equivalent to lumped capacitances C_{eq1} and C_{eq2} when they are reverse-biased, respectively.

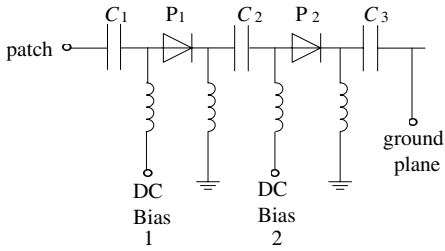

Figure 2. DC bias scheme for PIN diodes.

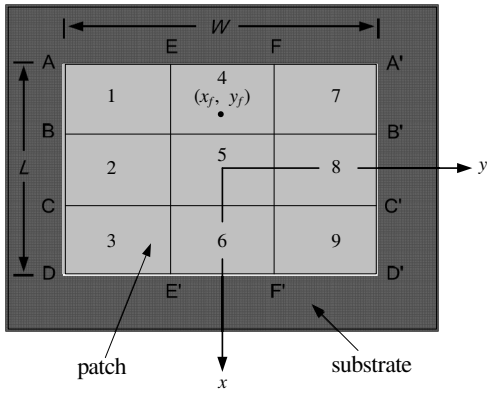

Figure 3. Partition diagram of the patch.

3.2. RCS Reduction Using PIN Diodes

To realize the RCS reduction, RF resistance characteristics of forward-biased PIN diodes are used to dissipate the field energy induced by an incident plane wave. Thus, the diodes are loaded at positions near where the maximum electric field occurs under the patch. Areas where the maximum electric field appears are determined by statistically analyzing distribution diagrams of the induced electric field under the patch. In order to locate the positions of the maximum electric field, the patch is divided into 9 areas, as shown in Fig. 3. In Fig. 3, $AB = BC = CD = L/3$, $AE = EF = FA' = W/3$. When we need the antenna at the low RCS state, we make PIN diodes present variable resistance characteristic by providing each diode a proper forward DC bias voltage. When we need the antenna at the optimal radiation state, we make PIN diodes present capacitance characteristic by applying a reverse DC bias voltage across each diode.

Three typical incident directions, i.e., ($\theta = 60°$, $\varphi = 0°$), ($\theta = 60°$, $\varphi = 90°$) and ($\theta = 60°$, $\varphi = 45°$), are studied in this paper. The

incident plane wave with θ-polarization, which means that the E-field polarization vector has only the θ component ($E_\theta = 1\,\mathrm{V/m}$, $E_\varphi = 0\,\mathrm{V/m}$), is used to illuminate the antenna from the three directions. For each incident angle, different modes are excited in antenna as the frequency of the incident wave changes. In this design, we observe the distribution diagrams of the electric field under the patch with a frequency interval of 0.05 GHz from 1 GHz to 8 GHz in order to study the resonant region scattering characteristics. Considering the fact that it is convenient to install the proposed diode bias circuit at the edge of the patch, we do not conduct statistics for Area 5.

3.2.1. ($\theta = 60°$, $\varphi = 0°$)

The observational results are shown in Table 1. m*1 in the table means that there are m frequency intervals in the corresponding frequency range listed in the left side, "1" denotes that the maximum electric field occurs within the corresponding area(s) listed in the above for each frequency interval. Area 1–9 can be sorted in terms of the occurrence number of the maximum electric field as frequency changes. According to statistics shown in Table 1, the sort result is $S_4 > S_7$, $S_1 > S_6 > S_9 > S_3 > S_2$, S_8 (where S_n denotes the occurrence number of the maximum electric field within n-th area with a frequency interval of 0.05 GHz). Based on the result, Area 4, Areas 4 and 7, Areas 4, 7 and 1, are loaded by PIN diodes for RCS reduction, respectively, corresponding results are shown in Fig. 4. From these results, it can be found that RCS reduction is not obviously improved until loading the antenna at Area 4, 7, 1 and 6, in such case RCS peaks at 2.54 GHz, 4.72 GHz and 7 GHz are reduced by 21.5 dB, 8.5 dB and 10.2 dB, respectively, compared to that of reference antenna. Thus we take Area 4, 7, 1 and 6 as loading positions for ($\theta = 60°$, $\varphi = 0°$), which is shown in Fig. 5. The optimized resistances at every loading position are $R_{eq1} = 60\,\Omega$ and $R_{eq2} = 220\,\Omega$, the lumped capacitances in bias network are $C_1 = 5\,\mathrm{pF}$, $C_2 = 0.5\,\mathrm{pF}$ and $C_3 = 15\,\mathrm{pF}$.

3.2.2. ($\theta = 60°$, $\varphi = 90°$)

The antenna is illuminated by a plane wave from the incident angle of ($\theta = 60°$, $\varphi = 90°$), and positions of the maximum electric field are shown in Table 2. The result is $S_3 > S_9 > S_1 > S_6 > S_2 > S_8 > S_4 > S_7$. The antenna is loaded at Area 3, Area 3 and 9, Area 3, 9 and 1, respectively, and the comparison of RCS results is shown in Fig. 6. RCS reduction is not obviously improved until loading the antenna at Area 3, 9, 1 and 6, in such case RCS peaks at 1.93 GHz, 4.02 GHz, 5.62 GHz and 7.29 GHz are reduced by 15 dB, 20.5 dB, 7.4 dB

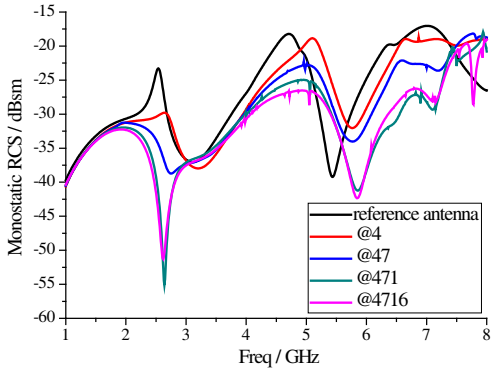

Figure 4. Monostatic RCS results for ($\theta = 60°$, $\varphi = 0°$).

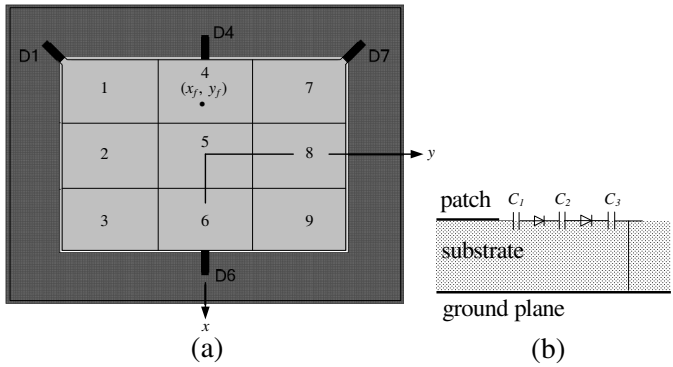

Figure 5. (a) The loading scheme for ($\theta = 60°$, $\varphi = 0°$). (b) The installation diagram of circuit components at each loading position.

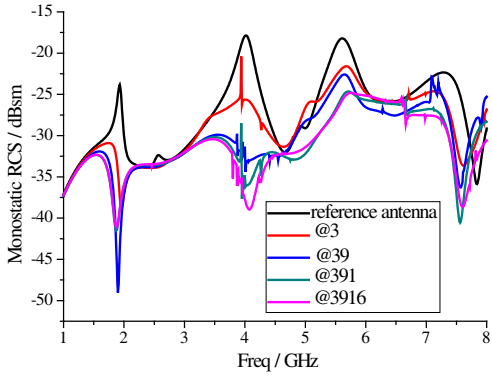

Figure 6. Monostatic RCS results for ($\theta = 60°$, $\varphi = 90°$).

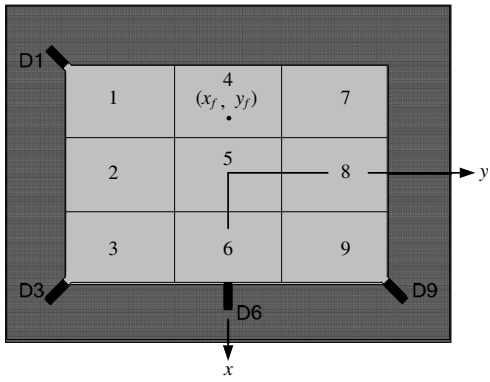

Figure 7. The loading scheme for ($\theta = 60°$, $\varphi = 90°$).

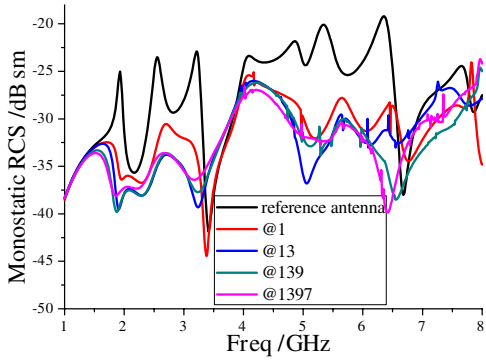

Figure 8. Monostatic RCS results for ($\theta = 60°$, $\varphi = 45°$).

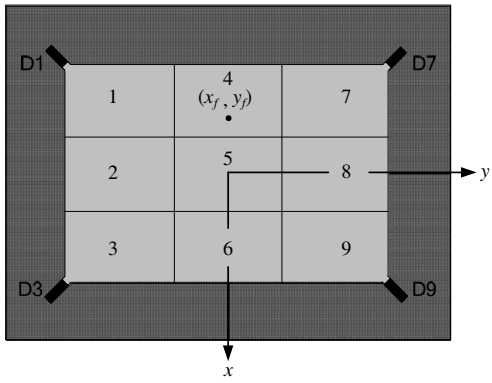

Figure 9. The loading scheme for ($\theta = 60°$, $\varphi = 45°$).

and 6.4 dB, respectively, compared with that of the reference antenna. Thus we take Areas 3, 9, 1 and 6 as loading positions for ($\theta = 60°$, $\varphi = 90°$), as shown in Fig. 7. The optimized resistance values are $R_{eq1} = 60\,\Omega$ and $R_{eq2} = 220\,\Omega$, and the lumped capacitances in bias network are $C_1 = 5\,\text{pF}$, $C_2 = 0.5\,\text{pF}$ and $C_3 = 15\,\text{pF}$.

Table 1. Statistics of distribution areas of the maximum electric field for ($\theta = 60°$, $\varphi = 0°$).

area / f(GHz)	1	2	3	4	6	7	8	9
1.8 – 1.95					4*1			
2 – 2.1				3*1				
2.15 – 2.3	4*1			4*1		4*1		
2.35 – 2.75	9*1		9*1	9*1	9*1	9*1		9*1
2.8 – 2.95	4*1			4*1		4*1		
3 – 3.05				2*1				
3.1				1	1			
3.2 – 4		17*1		17*1	17*1		17*1	
4.05		1	1	1	1		1	1
4.1 – 4.6			11*1					11*1
4.65 – 4.7	2*1		2*1		2*1	2*1		2*1
4.75	1				1	1		
4.8	1			1	1	1		
4.85	1			1		1		
4.9 – 4.95				2*1				
5.05				1	1			
5.1	1			1	1	1		1
5.2	1	1		1	1	1	1	1
5.2 – 6.1				19*1	19*1			
6.25	1	1	1	1	1	1	1	1
6.3 – 6.6	7*1	7*1	7*1			7*1	7*1	7*1
6.65 – 6.8	4*1	4*1				4*1	4*1	
6.85 – 7.4	12*1			12*1		12*1		
7.45 – 7.55	3*1		3*1	3*1		3*1		3*1
7.6 – 8	9*1		9*1			9*1		9*1
subtotal	60	31	43	83	59	60	31	45

Table 2. Statistics of distribution areas of the maximum electric field for ($\theta = 60°$, $\varphi = 90°$).

area / f(GHz)	1	2	3	4	6	7	8	9
1.8	1	1	1					1
1.85 – 2.1	6*1	6*1	6*1			6*1	6*1	6*1
2.15 – 2.3	4*1							
2.35 – 2.55	5*1				5*1	5*1		
2.6 – 3.45			18*1					18*1
3.5 – 4.25			16*1	16*1	16*1			16*1
4.3 – 4.65		8*1	8*1		8*1			8*1
4.7 – 4.85			4*1		4*1			4*1
4.9		1			1			1
4.95 – 5.15				5*1		5*1		
5.2	1			1		1		
5.25	1			1				
5.3	1			1			1	
5.35 – 5.4	2*1		2*1					
5.45 – 5.6	4*1	4*1	4*1					
5.65 – 6		8*1	8*1					8*1
6.05 – 6.2		4*1			4*1			
6.25	1	1	1	1	1			
6.3 – 6.8	11*1		11*1		11*1			
6.85 – 7.6	16*1		16*1				16*1	
7.65 – 7.7	2*1	2*1	2*1				2*1	2*1
7.75	1	1						1
7.8		1						1
7.85 – 7.9		2*1			2*1			2*1
7.95		1	1		1		1	1
8		1	1	1	1		1	1
subtotal	56	41	99	26	54	17	27	70

3.2.3. ($\theta = 60°$, $\varphi = 45°$)

Similarly, when the incident angle is ($\theta = 60°$, $\varphi = 45°$), statistical data are listed in Table 3 and the result is $S_1 > S_3 > S_9 > S_7 > S_2 > S_4 > S_6 > S_8$. According to the comparison of RCS results shown in Fig. 8, loading the antenna at Area 1, 3, 9 and 7 realizes a good RCS reduction within the observed frequency range. RCS

Table 3. Statistics of distribution areas of the maximum electric field for ($\theta = 60°$, $\varphi = 45°$).

area / f(GHz)	1	2	3	4	6	7	8	9
1.8	1					1		
1.85 – 2.05	5*1	5*1	5*1			5*1	5*1	5*1
2.1 – 2.35	6*1							
2.4	1		1					
2.45 – 2.6	4*1		4*1	4*1	4*1	4*1		
2.65 – 2.7	2*1		2*1					
2.75	1		1					1
2.8 – 3.5	15*1		15*1			15*1		15*1
3.55 – 4.05			11*1			11*1		
4.1			1		1	1		1
4.15 – 4.3				4*1	4*1			4*1
4.35 – 4.5				4*1	4*1			
4.55 – 4.65			3*1	3*1				
4.7 – 4.8	3*1		3*1	3*1				3*1
4.85 – 4.9	2*1		2*1	2*1		2*1		2*1
4.95 – 5	2*1			2*1	2*1	2*1		
5.05 – 5.1	2*1							
5.15 – 5.3	4*1	4*1	4*1					
5.35 – 5.4	2*1	2*1	2*1			2*1	2*1	2*1
5.45 – 5.6	4*1	4*1	4*1					
5.65 – 5.75	3*1		3*1					
5.8 – 5.85	2*1		2*1					2*1
5.9 – 6.35	10*1							10*1
6.4						1		
6.45					1			1
6.5 – 6.9	9*1	9*1		9*1	9*1	9*1	9*1	9*1
6.95		1	1					1
7 – 7.25		6*1	6*1					6*1
7.3 – 7.6			7*1					
7.65 – 7.85	5*1	5*1	5*1			5*1		5*1
7.9 – 8	3*1	3*1		3*1				
subtotal	86	39	82	34	25	58	16	67

peaks at 1.93 GHz, 2.55 GHz, 3.22 GHz, 4.08 GHz, 4.85 GHz, 5.35 GHz, 6.36 GHz and 7.66 GHz are reduced by 12.5 dB, 10.7 dB, 13.4 dB, 3.9 dB, 9.3 dB, 12.3 dB, 19.7 dB and 3 dB, respectively. Thus we take Area 1, 3, 9 and 7 as loading positions for ($\theta = 60°$, $\varphi = 45°$), as shown in Fig. 9. The optimized resistances are $R_{eq1} = 60\,\Omega$ and $R_{eq2} = 220\,\Omega$, and the lumped capacitances in bias network are $C_1 = 5\,\text{pF}$, $C_2 = 0.5\,\text{pF}$ and $C_3 = 15\,\text{pF}$.

4. COMBINATION OF THREE LOADING SCHEMES

Based on the above analysis for ($\theta = 60°$, $\varphi = 0°$), ($\theta = 60°$, $\varphi = 90°$) and ($\theta = 60°$, $\varphi = 45°$), we combine the loading schemes shown in Fig. 5, Fig. 7 and Fig. 9 in order to realize RCS reduction simultaneously for that three incident directions. The final loading scheme is shown in Fig. 10, capacitor values at each loading position and equivalent RF resistance values of all the loaded PIN diodes which are forward-biased are the same as aforementioned. Corresponding RCS results are compared with that of the reference antenna in Fig. 11.

As shown in Fig. 11(a), when the incident angle is ($\theta = 60°$, $\varphi = 0°$), RCS peaks at 2.54 GHz, 4.72 GHz and 7 GHz are reduced by 20 dB, 12.7 dB and 8.3 dB, respectively. When the incident angle is ($\theta = 60°$, $\varphi = 90°$), as shown in Fig. 11(b), RCS peaks at 1.93 GHz, 4.02 GHz, 5.62 GHz and 7.29 GHz are reduced by 12.5 dB, 21.7 dB, 7.2 dB and 6.6 dB, respectively. When the incident angle is ($\theta = 60°$, $\varphi = 45°$), as shown in Fig. 11(c), RCS peaks at 1.93 GHz, 2.55 GHz, 3.22 GHz, 4.08 GHz, 4.85 GHz, 5.35 GHz, 6.36 GHz and 7.66 GHz are reduced by 13.2 dB, 11.7 dB, 13.4 dB, 5.2 dB, 7 dB, 9.3 dB, 21.8 dB and 2.3 dB, respectively. Through the combination of loading schemes, RCS is obviously reduced within the observed frequency range for all the three incident angles.

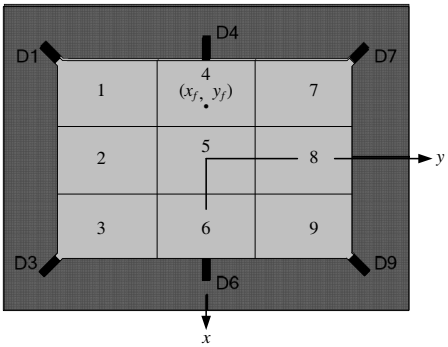

Figure 10. The combined loading scheme.

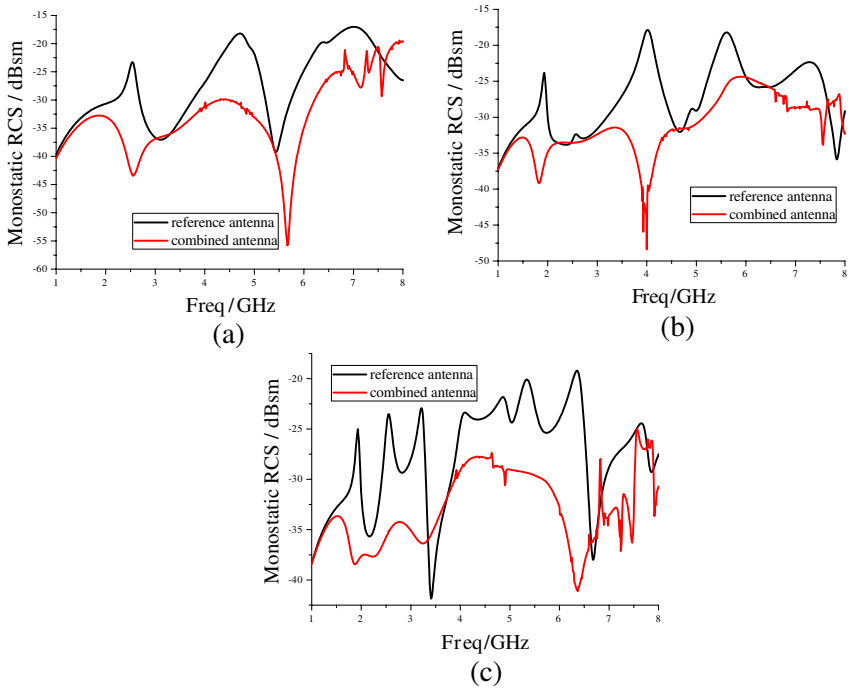

Figure 11. Comparison of monostatic RCS results between the reference antenna and the antenna with the combined loading scheme. (a) ($\theta = 60°$, $\varphi = 0°$). (b) ($\theta = 60°$, $\varphi = 90°$). (c) ($\theta = 60°$, $\varphi = 45°$).

5. RADIATION PERFORMANCES

When the antenna shown in Fig. 10 is in service, we let all the loaded PIN diodes present capacitance characteristics by applying a reverse DC bias voltage across each diode in order to maintain optimal radiation performances. During the process of simulation, we take 0.15 pF as the typical value of both C_{eq1} and C_{eq2} [24]. Although two cascaded diodes are used to decrease the total cascaded capacitance, there is a resonant frequency shift occurs. In order to compare antenna performances at the same operating frequency, L is only decreased by 2.7 mm to ensure the antenna shown in Fig. 10 operates at 2.5 GHz. Comparisons of performances between the antenna with the combined loading scheme and the reference antenna are shown in Fig. 12 and Fig. 13. The realized gain of the loaded antenna is 7.54 dBi, the relative bandwidth with S_{11} less than -10 dB is 4%. Compared with the reference antenna, the realized gain is reduced only by 0.17 dB, the bandwidth is reduced only by 0.2%, and the back lobe of the loaded antenna is increased by 1.5 dB.

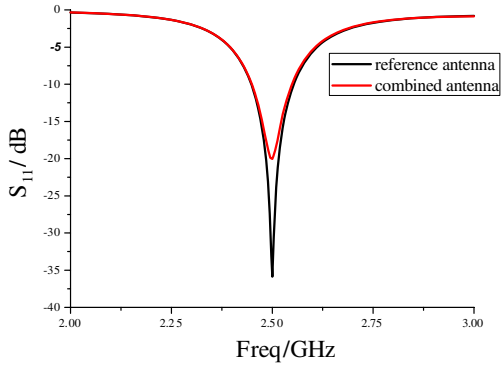

Figure 12. Comparison of S_{11} between the reference antenna and the loaded antenna.

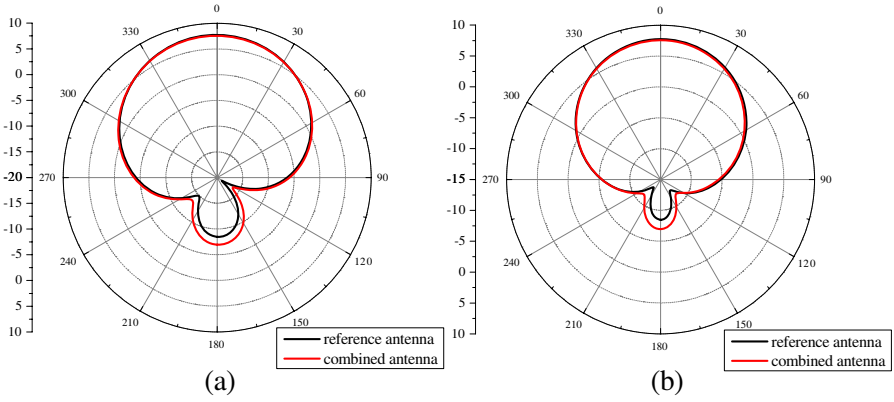

Figure 13. Comparison of radiation patterns at 2.5 GHz between the reference antenna and the antenna with the combined loading scheme. (a) E-plane. (b) H-plane.

6. CONCLUSION

A simple loading circuit is proposed in order to realize RCS reduction for a rectangular microstrip antenna using PIN diodes. By using the characteristics of on-resistance and off-capacitance of PIN diodes at RF frequencies, electronically switching the antenna between the optimal radiation state and the low RCS state is realized. Compared with the reference antenna, the radiation performances are well maintained when the loaded antenna is in service. Moreover, obvious RCS reduction is obtained over a large angular spatial region when we need the antenna at low RCS state.

ACKNOWLEDGMENT

This work was supported by National Natural Science Foundation of China under Grant No. 60971029 and National Defense Research Funding of China under Grant 10DZ0211.

REFERENCES

1. Vedaprabhu, B. and K. J. Vinoy, "An integrated wideband multifunctional antenna using a microstrip patch with two U-slots," *Progress In Electromagnetics Research B*, Vol. 22, 221–235, 2010.
2. Zhang, Y., B.-Z. Wang, W. Shao, W. Yu, and R. Mittra, "Artificial ground planes for performance enhancement of microstrip antennas," *Journal of Electromagnetic Waves and Applications*, Vol. 25, No. 4, 597–606, 2011.
3. Jackson, D. R., "The RCS of a rectangular microstrip patch in a substrate-superstrate geometry," *IEEE Trans. on Antenna and Propagation*, Vol. 38, No. 1, 2–8, 1990.
4. Wilsen, C. B. and D. B. Davidson, "The radar cross section reduction of microstrip patches," *IEEE Africon 4th*, Vol. 2, No. 1, 730–733, 1996.
5. Pozar, D. M., "RCS reduction for a microstrip antenna using a normally biased ferrite substrate," *Microwave and Guided Wave Letters*, Vol. 2 No. 5, 196–198, 1992.
6. H.-Y. Yang, J. A. Castaneda, and N. G. Alexopoulos, "Multifunctional antennas with low RCS," *Antennas and Propagation Society International Symposium*, Vol. 4, 2240–2243, 1992.
7. Volakis, J. L., A. Alexanian, and J. M. Lin, "Broadband RCS reduction of rectangular patch by using distributed loading," *Electronics Letters*, Vol. 28, 2322–2323, 1992.
8. Yang, H. and S. Gong, "RCS reduction technique out of operation of microstrip antennas," *Journal of Microwaves*, Vol. 20, No. 1, 35–39, 2004.
9. Ma, H., C. Xu, and H. Zheng, "Effect of impedance load on radiation and scattering of microstrip antenna," *Modern Electronic Technology*, Vol. 6, 6–7, 2004.
10. Zhao, S.-C., B.-Z. Wang, and Q.-Q. He, "Broadband radar cross section reduction of a rectangular patch antenna," *Progress In Electromagnetics Research*, Vol. 79, 263–275, 2008.

11. Zhao, S.-C., B.-Z. Wang, and W. Shao, "Reconfigurable Yagi-Uda substrate for radar cross section reduction of patch antenna," *Progress In Electromagnetics Research B*, Vol. 11, 173–187, 2009.
12. Xu, H.-Y., H. Zhang, X. Yin, and K. Lu, "Ultra-wideband koch fractal antenna with low backscattering cross section," *Journal of Electromagnetic Waves and Applications*, Vol. 24, Nos. 17–18, 2615–2623, 2010.
13. Zhu, X., W. Shao, J.-L. Li, and Y. Dong, "Design and optimization of low RCS patch antennas based on a genetic algorithm," *Progress In Electromagnetics Research*, Vol. 122, 327–339, 2012.
14. Jiang, W., T. Hong, Y. Liu, S.-X. Gong, Y. Guan, and S. Cui, "A novel technique for radar cross section reduction of printed antennas," *Journal of Electromagnetic Waves and Applications*, Vol. 24, No. 1, 51–60, 2010.
15. Hong, T., L.-T. Jiang, Y.-X. Xu, S.-X. Gong, and W. Jiang, "Radiation and scattering analysis of a novel circularly polarized slot antenna," *Journal of Electromagnetic Waves and Applications*, Vol. 24, No. 13, 1709–1720, 2010.
16. Ren, L.-S., Y.-C. Jiao, J.-J. Zhao, and F. Li, "RCS reduction for a FSS-backed reflectarray using a ring element," *Progress In Electromagnetics Research Letters*, Vol. 26, 115–123, 2011.
17. Aberle, J. T., M. Chu, and C. R. Birtcher, "Scattering and radiation properties of varactor-tuned microstrip antennas," *AP-S*, Vol. 4, 2229–2232, 1992.
18. Janaswamy, R. and S.-W. Lee, "Scattering from dipoles loaded with diodes," *IEEE Trans. on Antenna and Propagation*, Vol. 36, No. 11, 1649–1651, 1988.
19. Bai, Y.-Y., S. Q. Xiao, M.-C. Tang, et al., "Wide-angle scanning phased array with pattern reconfigurable elements," *IEEE Trans. on Antenna and Propagation*, Vol. 59, No. 11, 4071–4076, 2011.
20. Lin, S.-Y., Y.-C. Lin, and J.-Y. Lee, "T-strip FED patch antenna with reconfigurable polarization," *Progress In Electromagnetics Research Letters*, Vol. 15, 163–173, 2010.
21. Jamlos, M. F., O. A. Aziz, T. B. A. Rahman, M. R. B. Kamarudin, P. Saad, M. T. Ali, and M. N. Md Tan, "A reconfigurable radial line slot array (RLSA) antenna for beam shape and broadside application," *Journal of Electromagnetic Waves and Applications*, Vol. 24, Nos. 8–9, 1171–1182, 2010.
22. Raedi, Y., S. Nikmehr, and A. Poorziad, "A novel bandwidth enhancement technique for X-band RF MEMS actuated recon-

figurable reflectarray," *Progress In Electromagnetics Research*, Vol. 111, 179–196, 2011.

23. Vendelin, G. D., A. M. Pavio, and U. L. Rohde, *Microwave Circuit Design Using Linear and Nonlinear Techniques*, Ch. 12, Ch. 3, John Wiley & Sons, Inc., New Jersey, 2005.
24. Zhou, B. and G.-Z. Lu, "RF PIN diode switch in reconfigurable antenna," *Journal of Communication University of China (Science and Technology)*, Vol. 16, No. 4, 35–38, 2009.